Energy Aware Aerial Surveillance for a Long Endurance Solar-Powered UAV

Saghar Hosseini*, Mehran Mesbahi†
William E. Boeing Department of Aeronautics and Astronautics,
University of Washington, Seattle, WA 98195

In this paper, the energy optimal trajectories for Unmanned Aerial Vehicles (UAV) surveillance are explored. The main objective is to have maximum sensor coverage range while maintaining a perpetual flight. A solar powered UAV is used in this paper that is equipped with photovoltaic cells mounted on its wing and rechargeable batteries. The photovoltaic cells generate solar energy based on the position of the sun, attitude of the UAV, and sky clarity. The vehicle tries to optimize the energy storage in the batteries during the day. However, the sensor resolution diminishes due to altitude gain. A model for optimal coverage, path planning, and power allocation in a solar powered UAV is proposed and the corresponding simulation results are presented.

Nomenclature

ϕ	Bank angle, rad	L	Lift force, N
ψ	Heading angle, rad	C_L	Coefficient of lift
γ	Flight path angle, rad	D	Drag force, N
a	Azimuth of the sun, rad	C_D	Coefficient of drag
e	Elevation of the sun, rad	C_{D0}	Parasitic drag coefficient
i	Incidence angle of sun rays, rad	T	Thrust force, N
θ	Sensor field of view angle, rad	ϵ	Oswald efficiency factor
c	Sensor coverage range, m	g	Gravitational acceleration, m/s^2
x	x coordinate in a flat Earth-fixed reference frame, m	ρ	Air density, kg/m^3
y	y coordinate in a flat Earth-fixed reference frame, m	P_{batt}	Battery pack output power, $watt$
z	z coordinate in a flat Earth-fixed reference frame, m	Q	Battery pack charge capacity, Ah
V	Flight speed, m/s	V_{oc}	Battery pack open circuit voltage, $Volt$
n_v	Vertical load factor	R	Battery pack internal resistance, ohm
n_h	Horizontal load factor	SOC	Battery pack state of charge, %
η_{prop}	Efficiency of the propeller	P_{Tot}	Total power, $watt$
η_{sol}	Efficiency of the solar cells	P_{sd}	Solar spectral density, $watt/m^2$

I. Introduction

Long endurance Unmanned Aerial Vehicles (UAVs) have a wide range of applications in scientific research, crop and forestry fire monitoring, search and rescue, remote sensing, mapping, and atmospheric sensing missions. One way to extend the duration of UAV flight is to change the configuration of aircraft i.e. its wings[1] or propulsion system . In this context, hybrid propulsion systems with several power sources such as solar cells, fuel cells, and batteries have been proposed.[2,3] Another approach to increase the flight duration is to take advantage of energy available in the surrounding atmosphere in the form of wind gusts and thermals. There is extensive literature on path planning and trajectory optimization for soaring flight.[4–6] In addition, solar energy is a favorable candidate to collect energy

*Graduate Student, William E. Boeing Department of Aeronautics and Astronautics, University of Washington, Seattle, WA. Email: saghar@u.washington.edu
†Professor, William E. Boeing Department of Aeronautics and Astronautics, University of Washington, Seattle, WA. Email: mesbahi@aa.washington.edu

from the environment and power the UAVs. In pursuit of this goal, several solar powered UAVs have been built and flown since 1974. The latest solar powered UAV, Solar Eagle developed by Boeing, has an approximately 400 ft wingspan and is expected to be launched in 2014 to fly at high altitudes with an endurance of five years.

Provided with long endurance UAVs, the surveillance problem in aerial vehicles is becoming feasible and is an interesting research topic.[7–11] However, the energy efficiency aspect of this problem has not been addressed at large by scientific community. Mei et al.[12] proposed an efficient algorithm for deployment of multiple mobile robots that take into account energy and timing constraints, and explores the surveillance problem in ground robots. An endurance constraint is also considered in the aerial surveillance problem. Nigam et al.[13] added the endurance constraint to the control of multiple quad-rotor vehicles in order to achieve persistent surveillance. Moreover, Sujit and Ghose[14] presented a search algorithm for UAVs with limited fuel. These works does not deal with energy consumption constraint directly and use a fixed flight time to represent this constraint.

In energy optimal surveillance, the solar powered UAV employs optimal strategies to maximize energy harvesting and sensor coverage range during the flight. The energy optimized path planning problem for a solar powered UAV has been studied before.[15–19] For example, in our previous work,[15] we used model reduction techniques to investigate the optimal path planning and energy allocation problem for a single UAV in 3D space. The objective function was chosen as the final state of charge of the battery pack to maximize the energy stored on the UAV.

In this paper, we examine the optimal energy and coverage surveillance for a duration of 24 hours of a single solar powered UAV in 3D space. While maximizing the sensor coverage range for better observation, the secondary objective of the vehicle is to maximize the total energy stored in batteries at the end of the duration. During the mission, the aircraft must also satisfy boundary conditions and feasibility constraints on its states. Finally, a direct optimization method is used to solve the optimal energy surveillance problem and the results are compared with the optimal coverage surveillance problem.

The paper is organized as follows. §II presents the models for aircraft kinematics, power subsystems, and sensors. In §III, the optimal control problem formulations for two different objective functions are presented and a solution strategy based on nonlinear programming is discussed. Numerical results for a sample UAV path planning are investigated and their interpretation is described in §IV. Finally, §V presents the concluding remarks followed by future research.

II. Background and Model

This section presents a brief background on the models for the aircraft kinematics, electric components, and sensor coverage range used in this paper. The major power systems considered in the solar UAV are the solar cells, electric motor, and rechargeable batteries. The solar UAV power system generally contains other units of which power consumption is negligible compared to the three major components mentioned above.

A. Sensor Coverage Range

The sensor coverage range and resolution is modeled as a linear function of altitude as mentioned in Ref.[7] The sensor has a constant field of view angle and its coverage range increases as the UAV gain altitude. Nevertheless, the sensor resolution diminishes at high altitudes which is modeled as a linear function.

$$c(z) = \begin{cases} z \tan\theta & if\ 0 \le z \le h_{max} \\ h_{max} \tan\theta - \frac{h_{max} \tan\theta}{h_0 - h_{max}}(z - h_{max}) & if\ h_{max} \le z \le h_0 \end{cases}, \tag{1}$$

where c and z are the coverage range and altitude respectively. The sensor field of view angle is represented by θ. h_{max} is the altitude at which the sensor has maximum coverage range. Also, h_0 represents the altitude at which the sensor resolution is not appropriate for the aerial surveillance and without loss of generality we can assume the coverage range is zero at $z \ge h_0$. The coverage range of a sensor with a given field of view angle of θ is also shown in Fig. 1.

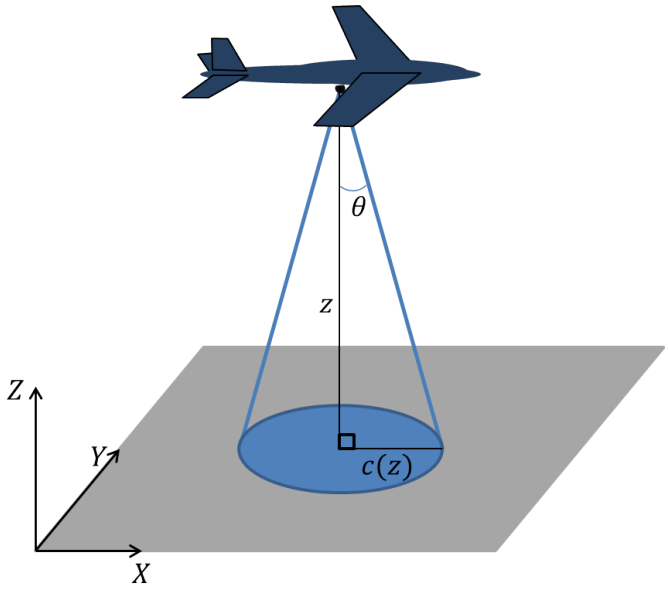

Figure 1. The sensor coverage range on the $X-Y$ plane.

The values of sensor parameters h_{max}, h_0, and θ used in numerical simulations are given in the appendix.

B. Electric Motor

Solar powered UAVs usually have an electric engine attached to a propeller. The output power consumed by the engine is defined as

$$P_{Eng} = \frac{TV}{\eta_{prop}}, \tag{2}$$

where T is the engine thrust and η_{prop} is the efficiency of the propeller. The available thrust is limited to a maximum value, T_{max}, which is predetermined by the characteristics of the aircraft engine.

C. Solar Cells

The power gained from photovoltaic cells is modeled based on the incidence angle with the sub, i, and solar cell parameters[17]

$$P_{Sun} = \eta_{sol} P_{sd} S \cos i, \tag{3}$$

where η_{sol} is the efficiency of the photovoltaic cells, S is the solar cell area, and P_{sd} is the solar spectral density. The incidence angle i depends upon the sun position in the sky and the UAV Euler angles. The sun position can be described by its azimuth and elevation angles as a function of time.[20] For example, the elevation and azimuth angles of the sun on a typical spring day in San Diego, California, is depicted in Fig. 2.

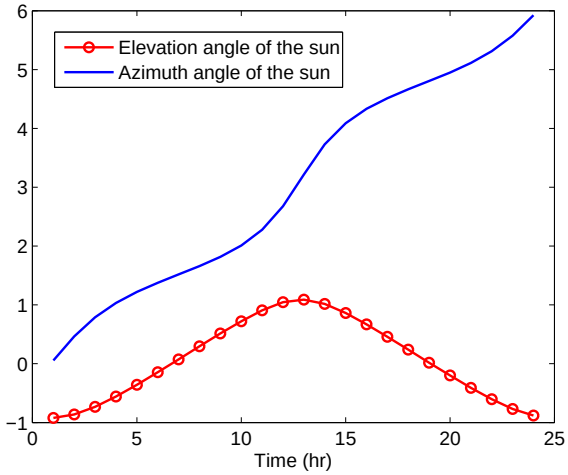

Figure 2. The azimuth and elevation angles of the sun on April 1st, 2012, in San Diego, CA. The simulation time starts at 1am and ends at midnight.

The inner product of the aircraft-fixed vertical axis and the sun position vector expressed in the aircraft-fixed frame yields cosine function for the incidence angle i,

$$\cos i = \hat{s}_A^T.z, \tag{4}$$

where $\hat{s_A}$ is the unit vector to the sun in the Earth-fixed frame and z is the aircraft-fixed vertical axis. The unit vector to the sun in aircraft-fixed frame can be expressed as

$$\hat{s_A}(t) = R_1(\phi)R_2(\gamma)R_3(\psi)\hat{s_E}(t). \tag{5}$$

The vector $\hat{s_E}$ in Eq. 5 is the unit vector to the Sun in the Earth-fixed frame defined as $\hat{s_E}(t) = [\cos e(t) \cos a(t) \;\; \cos e(t) \sin a(t)$ the R_1, R_2, and R_3 are rotation matrices about the first, second, and third axis, respectively. Figure 3 illustrates the Euler angles and the unit vector to the Sun in the Earth-fixed frame.

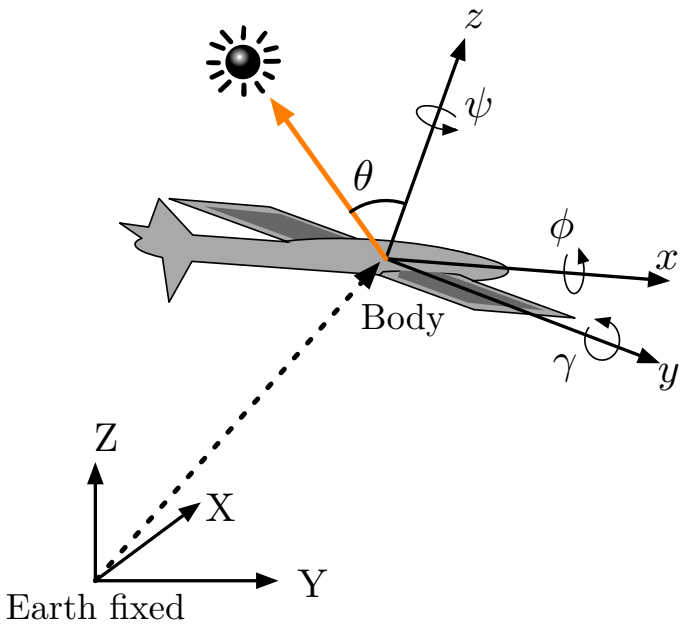

Figure 3. (X, Y, Z) represents the Earth-fixed frame and (x, y, z) represents the aircraft-fixed frame. The sun angles, i.e., a, e, are defined in the Earth-fixed frame and UAV Euler angles, i.e., γ, ϕ, and ψ are expressed in aircraft-fixed frame.

D. Rechargeable Battery Pack

The rechargeable battery pack stores solar power harvested by the photovoltaic cells and provides it to the electric motor. The battery pack output power is modeled based on the circuit representation of lithium-sulfur cells (Li-S)[21]

$$P_{Batt} = -V_{OC} Q S\dot{O}C - R(QS\dot{O}C)^2, \tag{6}$$

where V_{OC} is the battery pack open circuit voltage, R is the battery pack internal resistance, Q is the battery pack capacity, and SOC is the battery pack state of charge defined as the ratio of current charge capacity to maximum charge capacity. The battery specification sheet[22] implies that the open circuit voltage of the battery pack is a function of the cell temperature and the value of SOC. However, the impact of SOC is negligible under normal temperature and V_{OC} is assumed to be constant in this paper.

In order to optimize the limited cycle life of batteries[21], the SOC must satisfy

$$0.25 \leq SOC \leq 0.9. \tag{7}$$

In addition, the charge and discharge performance is bounded by the capability of battery pack as described in Eq. 8

$$P_{Batt_0,Charge} \leq P_{Batt} \leq P_{Batt_0,Discharge}. \tag{8}$$

Based on Eq. (6), the rate of charge of SOC can be represented as

$$\frac{d}{dt}SOC = -\frac{V_{OC} - \sqrt{V_{OC}^2 - 4P_{Batt}R}}{2QR}. \tag{9}$$

E. Aircraft Kinematics Model in Three Dimensions

The point mass aircraft kinematics in three dimensions are presented in this section. The aircraft flies in still air and its states are governed by the following equations[23]

$$\begin{gathered} \dot{x} = V\cos\psi\cos\gamma, \quad \dot{y} = V\sin\psi\cos\gamma, \quad \dot{z} = V\sin\gamma \\ \dot{\psi} = \frac{g}{V}\left(\frac{n_h}{\cos\gamma}\right), \quad \dot{\gamma} = \frac{g}{V}(n_v - \cos\gamma) \\ \dot{V} = \left(\frac{T-D}{mg} - \sin\gamma\right) g. \end{gathered} \tag{10}$$

The states x, y, and z are the aircraft position coordinates in a Earth-fixed reference frame, V is the aircraft velocity, ψ is the heading angle, and γ is the flight path angle. The forces D and T represent drag and thrust, respectively. The parameters n_v and n_h are the vertical and horizontal load factors defined as

$$n_h = \frac{L\sin\phi}{W}, \quad n_v = \frac{L\cos\phi}{W}, \tag{11}$$

where W represents the aircraft weight, and L represents lift force. The bank angle ϕ can be expressed as $\phi = \tan^{-1}\left(\frac{n_h}{n_v}\right)$ based on Eq. 11. Moreover, the standard lift and drag equations gives the drag force D in Eq. (10)

$$\begin{gathered} C_L = \frac{nW}{\frac{1}{2}\rho V^2 S}, \quad C_D = C_{D0} + KC_L^2 \\ D = \frac{1}{2}\rho V^2 S C_D, \end{gathered} \tag{12}$$

where C_L is the lift coefficient, C_D is the drag coefficient, C_{D0} is the coefficient of parasitic drag, and K is the aerodynamic coefficient. The parameter n is the magnitude of the load factor, which can be determined by n_h and n_v such that $n = \sqrt{n_h^2 + n_v^2}$. The air density ρ in Eq. 12 is estimated from the U.S. Standard Atmosphere.[24]

III. Problem Statement

In this section, the problem of energy optimal trajectories for surveillance between two given locations is formulated as an optimal control problem with a set of constraints. The cost function in the optimal coverage problem is the cumulative sum of sensor coverage range over time.

$$C(t_f) = \int_{t_0}^{t_f} c(z)dt, \tag{13}$$

where $c(z)$ is the coverage range given in Eq. 1. The final state of charge $SOC(t_f)$ in battery pack is also used as the cost function for energy optimal path planning.[15] The state variables $[x, y, z, \psi, \gamma, V, SOC, C]^T$ and control variables $[n_v, n_h, T, P_{Batt}]^T$are constrained to satisfy the aircraft kinematics in Eq. (10), battery discharge rate in Eq. (9), sensor coverage range in Eq. 1, and boundary conditions. The mission is to fly between the specified initial and final positions during the time interval $[t_0, t_f]$.

Several constraints on state and control variables are also introduced based on limited UAV maneuverability, structural capability, solar sources, and battery capacity. The UAV velocity is bounded by V_{stall} and V_{max} which are the stall and maximum feasible velocity of the aircraft, respectively. The rate of change of heading angle ψ has to satisfy $|\dot{\psi}| \leq \dot{\Psi}$ in order to generate a smooth trajectory where $\dot{\Psi}$ is the maximum changing rate of the heading angle. Powered flight requires the total power P_{Tot} to be positive, which means the power consumption must be less than or equal to power generated by solar cells and/or the battery pack. Based on the above description, the optimal energy surveillance problem can be formulated as:

$$\max_{(n_v, n_h, T, P_{Batt})} C(t_f) + SOC(t_f) \tag{14}$$

subject to

$$\begin{gathered}
\dot{x} = V\cos\psi\cos\gamma, \quad \dot{y} = V\sin\psi\cos\gamma, \quad \dot{z} = V\sin\gamma \\
\dot{\psi} = \frac{g}{V}\left(\frac{n_h}{\cos\gamma}\right), \quad \dot{\gamma} = \frac{g}{V}(n_v - \cos\gamma) \\
\dot{V} = \left(\frac{T-D}{mg} - \sin\gamma\right) g \\
\dot{SOC} = -\frac{V_{OC} - \sqrt{V_{OC}^2 - 4P_{Batt}R}}{2QR} \\
\dot{C} = c(z)
\end{gathered} \tag{15}$$

and

$$\begin{gathered}
||\dot{\psi}| \leq \dot{\Psi}, \ |\gamma| \leq \frac{\pi}{2}, \\
V_{stall} \leq V \leq V_{max}, \\
0 \leq T \leq T_{max}, \\
0.25 \leq SOC \leq 0.9, \\
|n_v| \leq n_{v_{max}}, \quad |n_h| \leq n_{h_{max}}, \\
P_{Batt_0,Charge} \leq P_{Batt} \leq P_{Batt_0,Discharge} \\
P_{Tot=}P_{Sun} + P_{Batt} - P_{Eng} \geq 0,
\end{gathered} \tag{16}$$

with boundary conditions:

$$\begin{gathered}
[x(t_0), y(t_0), z(t_0), \psi(t_0), \gamma(t_0), V(t_0), SOC(t_0)]^T = \\
[x_0, y_0, z_0, \psi_0, \gamma_0, V_0, SOC_0]^T \\
[x(t_f), y(t_f), z(t_f)]^T = [x_f, y_f, z_f]^T,
\end{gathered} \tag{17}$$

IV. Nonlinear Programming Approach

A. Nonlinear Programming Method

The optimal control problem presented in Eq. (14) through Eq. (17) is a complex nonlinear optimization problem and large in dimension. The general approach to solve these types of problems is the direct collocation (DC) method. DC is an approximate method that discretizes a continuous solution and uses linear interpolation to satisfy the differential equations. This method transforms the optimal control problem into a nonlinear programming problem (NLPP) and the solution is in terms of infinitely many values of state and control variables.

The nonlinear programming (NLP) solver used to solve our optimization problem is based on a sequential quadrature programming (SQP) algorithm called NPSOL.[25,26] NPSOL can be used to solve problems such as minimizing a performance index subject to constraints on individual state and/or control variables. Since the mission time of 24-hour is long (86400 seconds), some of the state and control variables need to be scaled to make the solution converge faster and also avoid the singularities that may occur in estimating the underlying Hessian matrices.

B. Simulation Results using NLP Method

The simulation results for the two optimal control problems are illustrated in this section and their corresponding sensor coverage and energy storage are compared. The boundary conditions are provided in Table 1. The UAV starts from the origin with zero heading and flight path angles and returns to its initial location after 24 hours. The mission endurance is discretized into 24 nodes representing each hour during one day and night. This large time step simplifies the optimization problem as well as providing fast convergence and smooth trajectories.

Table 1. Boundary conditions

States	Values
$[x_0, y_0, z_0]$ (km)	$[0, 0, 0]$
$[\psi_0, \gamma_0]$ (rad)	$[0, 0]$
V_0 (m/s)	V_{min}
SOC_0	0.9
$[x_f, y_f, z_f]$ (km)	$[0, 0, 0]$

C. Optimal Coverage Surveillance Problem

Figures 9 through 12 illustrate the numerical results for optimal coverage surveillance with the cost function specified in Eq. 13 where the energy storage in the system is not optimized. Figure 4(a) and Fig. 4(b) present the optimal trajectory in 3D space as well as its projection on the $X - Y$ plane. The optimal trajectory is relatively smooth based on the facts that the time step chosen in algorithm is 1 hour and the heading rate of change is constrained in the optimization problem.

Regarding the velocity and altitude profile in Figs. 5(a) and 5(b), the UAV velocity during the flight has small scale fluctuation around 10 m/s. In addition, the UAV starts at zero altitude and reaches $z \approx 500m$ altitude. The aircraft stays at that altitude at which the sensor coverage range is at its maximum value. Although, the goal of the UAV is to achieve maximum sensor coverage range, it has to maintain the powered flight. Therefore, the UAV climbs up to higher altitudes ($z \approx 2km$) to gain potential energy and spend this energy by soaring during night.

Figure 6 shows the smooth transitions of attitude angles of the UAV during trajectory. Figure 6(a) implies that the solar harvesting reaches maximum at noon and is zero between sunset and sunrise. Besides, the flight path angle γ shown in Fig. 6(c) is very small during the flight. It is noted in Fig. 6(c), the bank angle ϕ is approximately zero during the mission which refers to the fact that the aerodynamic drag value is at its local minimum when $\phi = 0$.[15]

Maintaining a powered flight is one of the optimization constraints as described in Eq. 16. Therefore, the power allocation strategy is illustrated in Fig. 7 for further investigation. Figure 7(a) indicates the time history of the SOC and Fig. 7(b) represents the power allocation during the trajectory. It is shown that the battery pack is charged during the day while the UAV uses solar power to supply the required power.

Finally, the coverage range of the UAV sensor is presented in Fig. 8, which demonstrates the UAV tendency to stay at a_{max}.

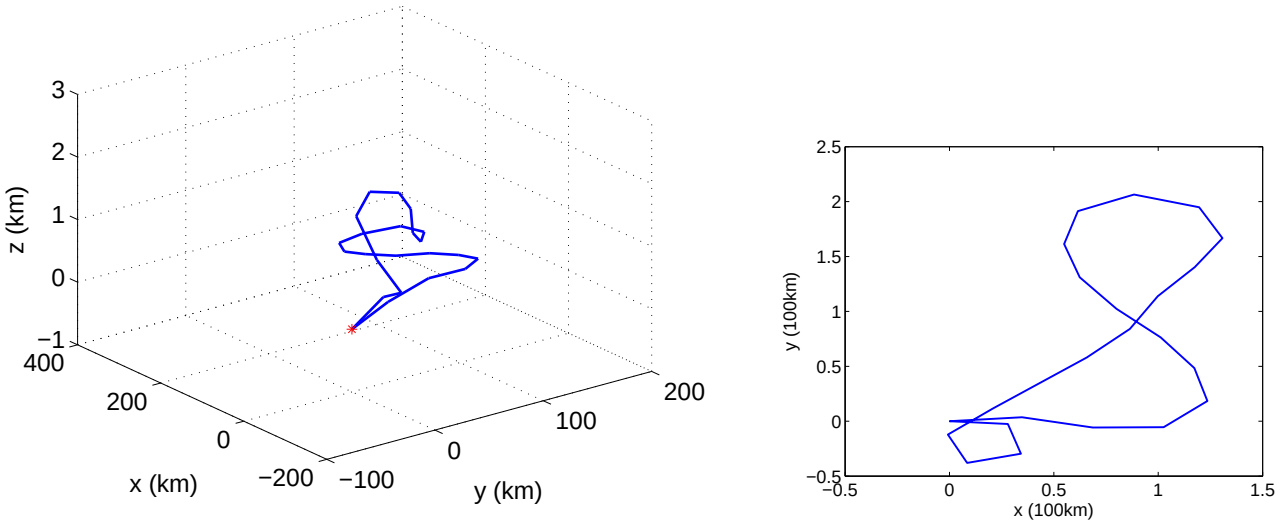

(a) (b)

Figure 4. The optimal trajectory in $(X-Y-Z)$ space (a), and the $X-Y$ plane (b) are depicted in these figures for the optimal coverage surveillance problem.

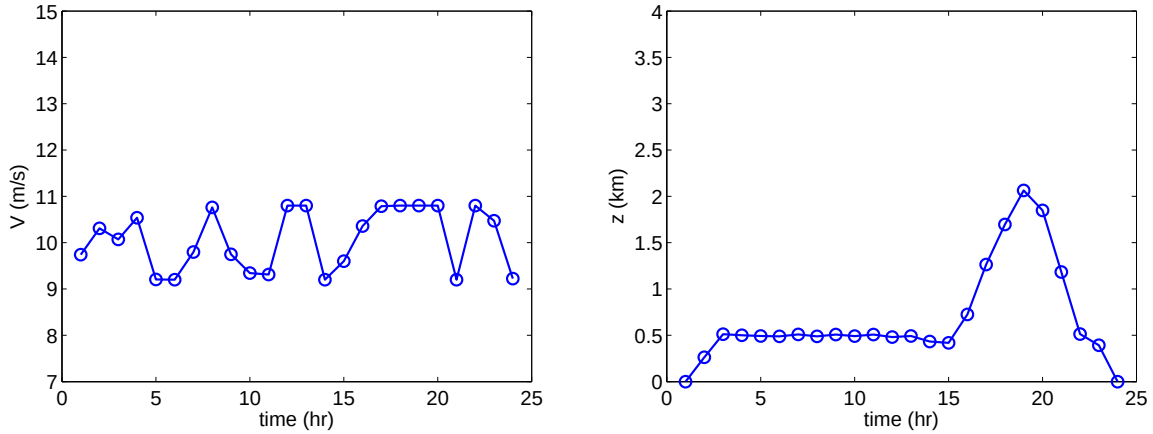

(a) (b)

Figure 5. (a) The UAV velocity during the trajectory, and (b) the altitude of UAV as a function of time are shown for the optimal coverage surveillance problem.

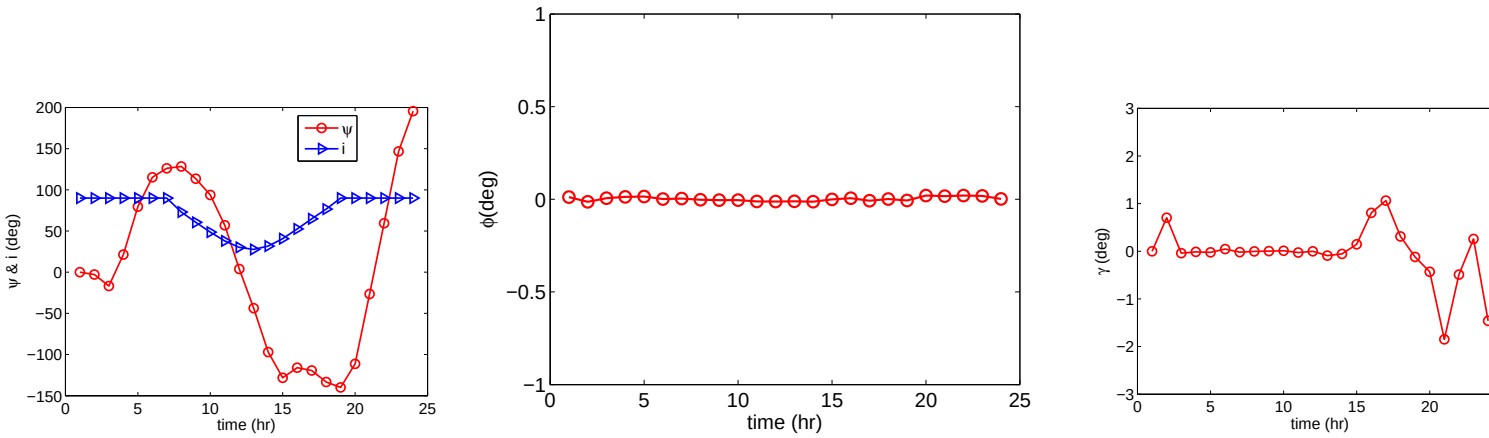

Figure 6. The aircraft attitude for the optimal coverage surveillance problem is represented by (a) the heading angle, ψ, sun incidence angle, i, (b) bank angle, ϕ, (c) and flight path angle, γ. The time span is from 1am to midnight of April 1, 2012.

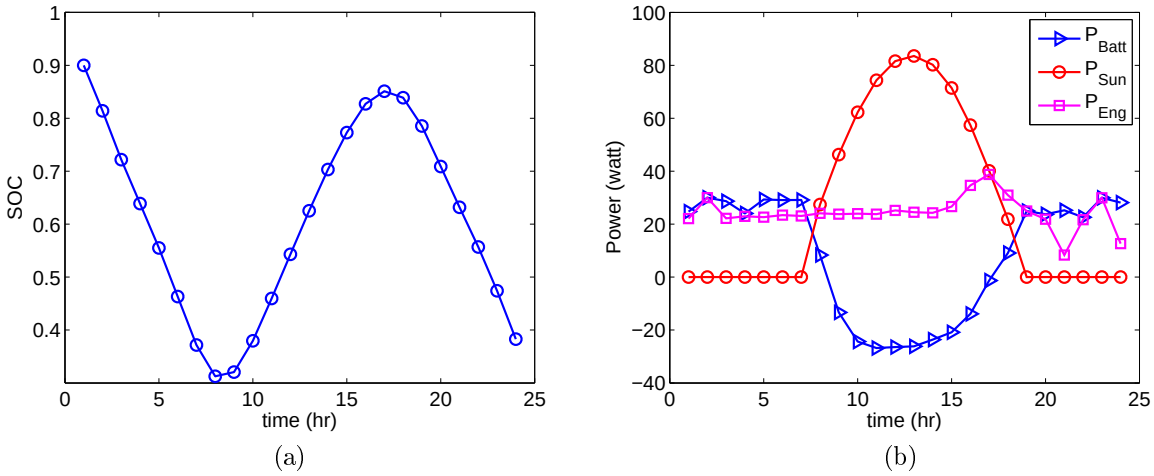

Figure 7. (a) Presents the SOC of the battery pack and (c) shows the optimal power allocation during the optimal trajectory for the optimal coverage surveillance problem.

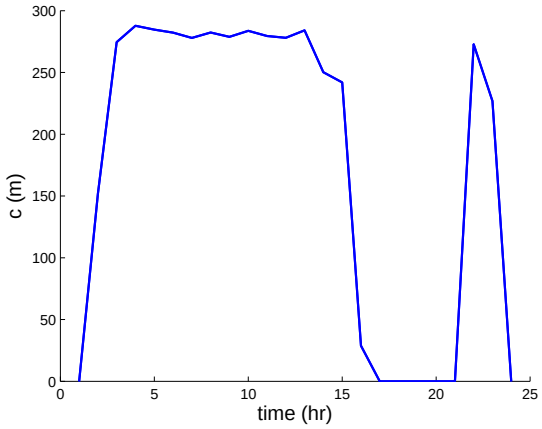

Figure 8. Sensor coverage range during the optimal trajectory for the optimal coverage surveillance problem.

The optimal coverage cost and final SOC in this scenario are

$$C(t_f) = 16226km, \quad SOC(t_f) = 0.383. \tag{18}$$

D. Optimal Energy Surveillance Problem

The objective function of the optimal energy surveillance problem is to maximize both the sensor coverage range and the final state of the charge for the battery pack which represents the energy stored in the system. The objective function for this optimal control problem is expressed in Eq. 14. The optimal trajectory and its velocity profile shown in Figs. 9 and 10 have slightly different properties than the optimal coverage problem results. In this case, the energy storage in the system has an important contribution to cost function. Therefore, the UAV climbs higher ($z \approx 3\ km$) in order to harvest more potential energy. The attitude of the UAV is shown by its Euler angles in Fig. 11. The Euler angles have also similar profiles as in the optimal coverage surveillance problem.

Moreover, the optimal power allocation strategy is shown in Fig. 12. Figure 12(a) indicates the time history of the SOC status from the optimal power allocation output. The SOC profile suggests that the rechargeable battery pack recovers most of its initial state of charge allowing the UAV to resume its operation the next day. The engine input power, as well as output power form battery pack and solar cells, are depicted in Fig. 12(b). It demonstrates how the engine operates during the early hours of the mission when UAV performs level flight at low altitude. The amount of power at this stage is approximately equivalent to the minimum power required at that altitude. In addition, the solar power from the sun compensates for both recharging the battery and supplying enough power for maintaining powered flight during the day. Notice in Fig. 12(b) that the total power P_{Tot} in (16) is non-negative at all time nodes satisfying the powered flight constraint. Lastly, the coverage range of UAV sensor is presented in Fig. 13 which has approximately the same profile as in the optimal coverage surveillance result.

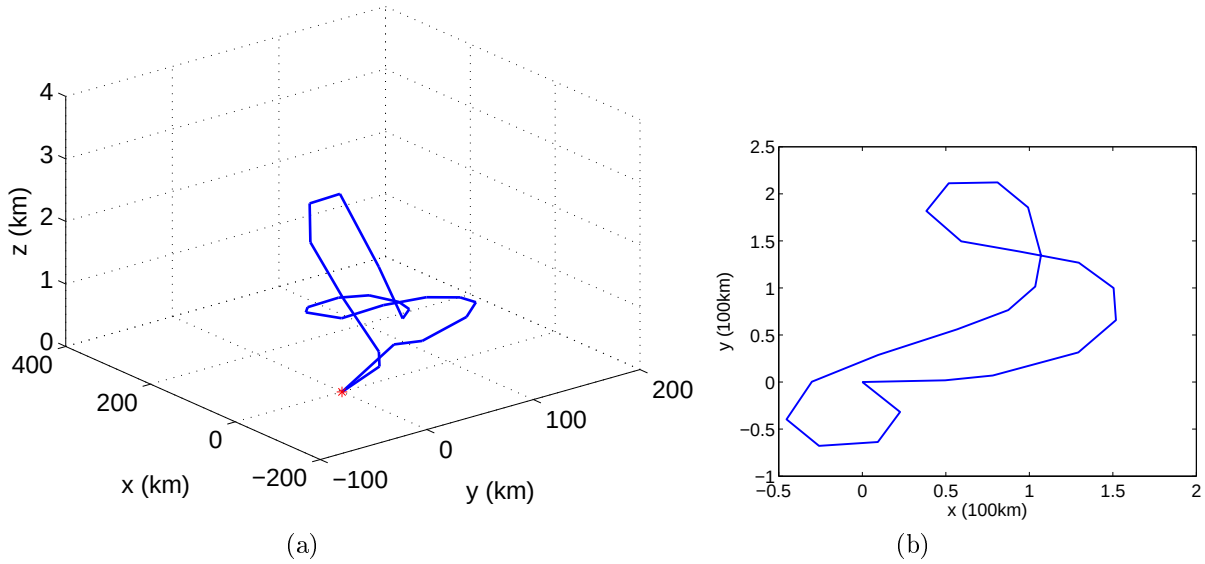

(a) (b)

Figure 9. The optimal trajectory in $X-Y-Z$ space (a), and the $X-Y$ plane (b) are depicted in these figures for the optimal energy surveillance problem.

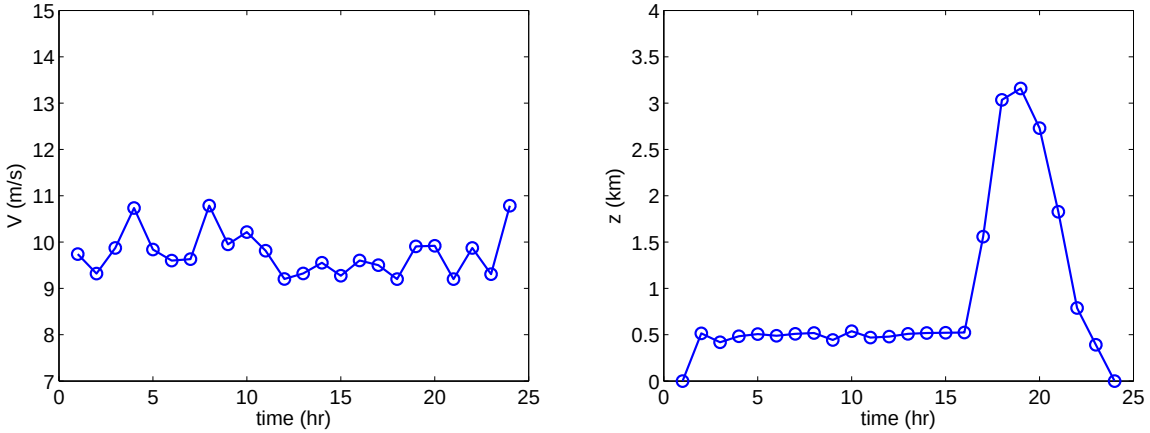

(a) (b)

Figure 10. The UAV velocity during the trajectory (a), and the altitude of UAV as a function of time (b) are shown in this figure for the optimal energy surveillance problem.

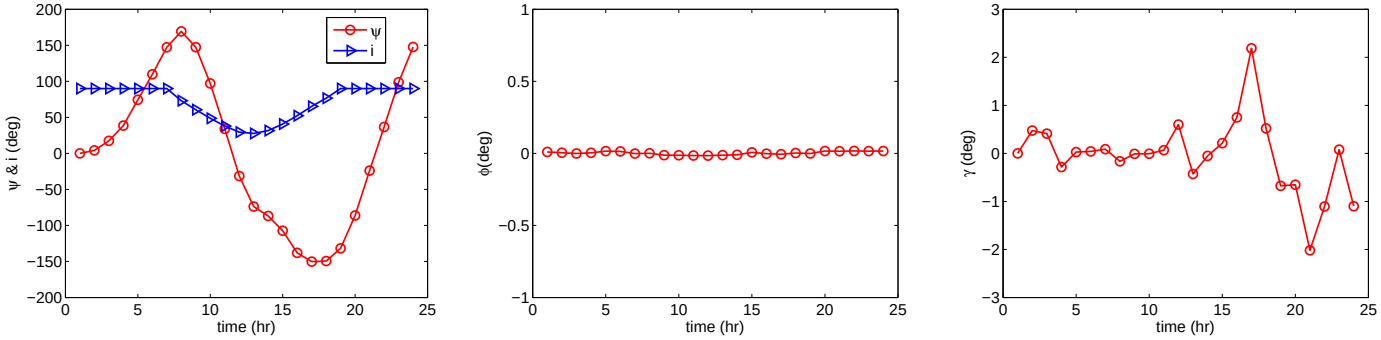

(a) (b) (c)

Figure 11. The aircraft attitude for the optimal energy surveillance problem is represented by (a) heading angle, ψ, Sun incidence angle, i, (b) bank angle, ϕ, (c) and flight path angle, γ. The time span is from 1am to midnight of April 1, 2012.

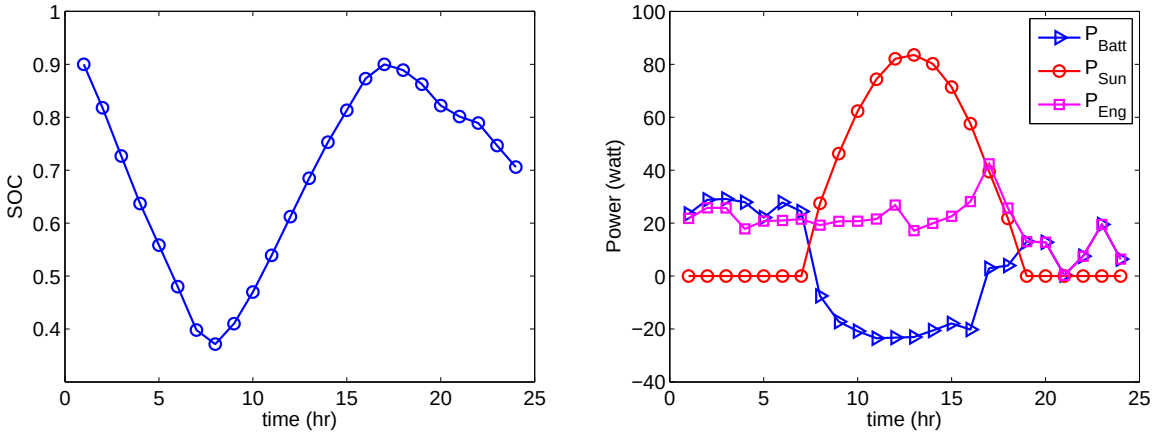

(a) (b)

Figure 12. Figure (a) presents the SOC of the battery pack and figure (b) shows the optimal power allocation during the optimal trajectory for the optimal energy surveillance problem.

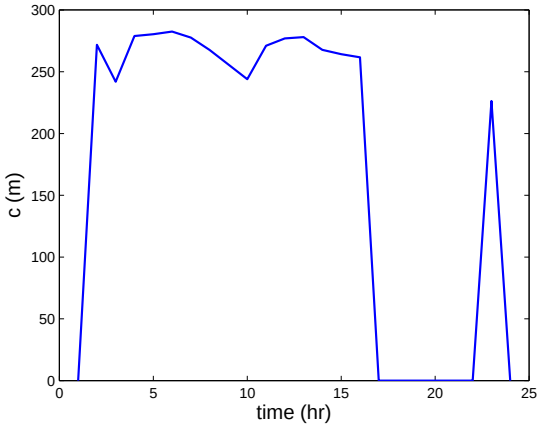

Figure 13. Sensor coverage range during the optimal trajectory for the optimal energy surveillance problem.

The optimal coverage cost and final SOC in this scenario are

$$C(t_f) = 16372km, \quad SOC(t_f) = 0.706. \tag{19}$$

From Eqs. 18 and 19 it is noted that the coverage range cost function $C(t_f)$ is slightly less than its value for the energy optimal surveillance problem. Moreover, the final SOC of the battery pack is improved by %84 which implies that the UAV can achieve a local optimal coverage while optimizing its energy storage. This property can also be used to design perpetual surveillance mission.

V. Conclusion

A simple model is proposed to formulate the optimal energy surveillance problem for a solar-powered UAV in 3D space. In this model, the sensor capabilities and electrical models are integrated with the aircraft kinematics when solving the optimization problem. The objective function for an optimal coverage surveillance problem is defined as the cumulative sum of coverage range over time. Periodic boundary conditions were considered for the numerical simulations and optimal solutions using nonlinear programming were obtained. The solutions provide complete information on the trajectory and power allocation strategy of the UAV. It was noted from the simulation results that the UAV mission is divided into three phases; level flight, climb, and descend. In the optimal energy surveillance problem, the final state of charge of the battery pack is included in the objective function. By comparing the simulation results for these two optimal control problems, it was shown that the energy stored in the UAV is optimized while keeping the same coverage range profile in the energy optimal surveillance problem. In addition, the trajectory properties are similar in these two cases. The altitude and SOC profiles suggest that the most effective contribution to saving energy is the potential energy harvested during climb phase.

This paper is an elementary step towards designing trajectories for long endurance solar powered UAVs which requires further investigations. The future research will focus on thermal soaring and the effect of wind gust on the UAV trajectory. Cooperative aerial surveillance and developing simple convex models to simplify this problem are also other problems which are appealing to explore.

References

[1]Meyer, J., du Plessis, J., Ellis, P., and Clark, W., "Design considerations for a low altitude long endurance solar powered unmanned aerial vehicle," Piscataway, NJ, USA, 2007//, pp. 1 – 6, solar powered unmanned aerial vehicle;low altitude long endurance unmanned aerial vehicle;low altitude long endurance flight;.

[2]Capata, R., Marino, L., and Sciubba, E., "A hybrid propulsion system for a high-endurance UAV: Configuration selection and aerodynamic study," Vol. 11, Denver, CO, United states, 2011, pp. 767 – 774.

[3]Chiesa, S., Farfaglia, S., Fioriti, M., and Viola, N., "Design of all electric secondary power system for future advanced medium altitude long endurance unmanned aerial vehicles," *Proceedings of the Institution of Mechanical Engineers, Part G: Journal of Aerospace Engineering*, Vol. 226, No. 10, 2012, pp. 1255 – 1270.

[4]Akos, Z., Nagy, M., Leven, S., and Vicsek, T., "Thermal Soaring Flight of Birds and Unmanned Aerial Vehicles," *Bioinspiration & Biomimetics*, Vol. 5, No. 4, 2010/12/, pp. 045003 (12 pp.) –.

[5]Langelaan, J. W., "Long distance/duration trajectory optimization for small UAVs," Vol. 4, Hilton Head, SC, United states, 2007, pp. 3654 – 3667.

[6]Kagabo, W. and Kolodziej, J., "Trajectory determination for energy efficient autonomous soaring," *American Control Conference (ACC), 2011*, 29 2011-july 1 2011, pp. 4655 –4660.

[7]Acevedo, J. J., Arrue, B. C., Maza, I., and Ollero, A., "Cooperative large area surveillance with a team of aerial mobile robots for long endurance missions," *Journal of Intelligent and Robotic Systems: Theory and Applications*, Vol. 70, No. 1-4, 2013, pp. 329 – 345.

[8]Doitsidis, L., Weiss, S., Renzaglia, A., Achtelik, M. W., Kosmatopoulos, E., Siegwart, R., and Scaramuzza, D., "Optimal surveillance coverage for teams of micro aerial vehicles in GPS-denied environments using onboard vision," *Autonomous Robots*, Vol. 33, No. 1-2, 2012, pp. 173 – 188.

[9]Beard, R., McLain, T., Nelson, D., Kingston, D., and Johanson, D., "Decentralized Cooperative Aerial Surveillance Using Fixed-Wing Miniature UAVs," *Proceedings of the IEEE*, Vol. 94, No. 7, july 2006, pp. 1306 –1324.

[10]Alexis, K., Nikolakopoulos, G., Tzes, A., and Dritsas, L., "Coordination of Helicopter UAVs for Aerial Forest-Fire Surveillance," *Applications of Intelligent Control to Engineering Systems*, edited by K. P. Valavanis, Vol. 39 of *Intelligent Systems, Control and Automation: Science and Engineering*, Springer Netherlands, 2009, pp. 169–193.

[11]Flint, M., Polycarpou, M., and Fernandez-Gaucherand, E., "Cooperative control for multiple autonomous UAV's searching for targets," *Decision and Control, 2002, Proceedings of the 41st IEEE Conference on*, Vol. 3, dec. 2002, pp. 2823 – 2828 vol.3.

[12]Mei, Y., Lu, Y.-H., Hu, Y., and Lee, C., "Deployment of mobile robots with energy and timing constraints," *Robotics, IEEE Transactions on*, Vol. 22, No. 3, june 2006, pp. 507 – 522.

[13]Nigam, N., Bieniawski, S., Kroo, I., and Vian, J., "Control of Multiple UAVs for Persistent Surveillance: Algorithm and Flight Test Results," *Control Systems Technology, IEEE Transactions on*, Vol. 20, No. 5, sept. 2012, pp. 1236 –1251.

[14]Sujit, P. and Ghose, D., "Search using multiple UAVs with flight time constraints," *Aerospace and Electronic Systems, IEEE Transactions on*, Vol. 40, No. 2, april 2004, pp. 491 – 509.

[15]Saghar Hosseini, R. D. and Mesbahi, M., "Optimal Path Planning and Power Allocation for a Long Endurance Solar-Powered UAV," *American Control Conference, June 17 - 19, Washington, DC*, 2013.

[16]Klesh, A. T. and Kabamba, P. T., "Energy-optimal path planning for Solar-powered aircraft in level flight," *AIAA Guidance, Navigation, and Control Conference 2007, August 20, 2007 - August 23*, Vol. 3, American Institute of Aeronautics and Astronautics Inc, 2007 2007, pp. 2966–2982.

[17]Klesh, A. T. and Kabamba, P. T., "Solar-powered aircraft: Energy-optimal path planning and perpetual endurance," *Journal of Guidance, Control, and Dynamics*, Vol. 32, No. 4, 2009, pp. 1320–1329.

[18]Spangelo, S. C., Gilberty, E. G., Klesh, A. T., Kabamba, P. T., and Girard, A. R., "Periodic energy-optimal path planning for solar-powered aircraft," *AIAA Guidance, Navigation, and Control Conference*, Chicago, IL, United states, August 2009.

[19]Sachs, G., Lenz, J., and Holzapfel, F., "Unlimited endurance performance of solar UAVs with minimal or zero electric energy storage," *AIAA Guidance, Navigation, and Control Conference*, Chicago, IL, United states, August 2009.

[20]Reda, I. and Andreas, A., "Solar position algorithm for solar radiation applications," *Solar Energy*, Vol. 76, No. 5, 2004, pp. 577–589.

[21]Moura, S. J., Callaway, D. S., Fathy, H. K., and Stein, J. L., "Tradeoffs between battery energy capacity and stochastic optimal power management in plug-in hybrid electric vehicles," *Journal of Power Sources*, Vol. 195, No. 9, 2010, pp. 2979 – 2988.

[22]http://sionpower.com/technology.html.

[23]Dai, R. and Jr., J. E. C., "Three-dimensional trajectory optimization in constrained airspace," *Journal of Aircraft*, Vol. 46, No. 2, 2009, pp. 627–634.

[24]U.S. Government Printing Office, Washington, D., "U.S. Standard Atmosphere," 1976.

[25]K. Holmstrom, A. G. and Edvall, M. M., "User's Guide For TOMLAB/SNOPT," 2005.

[26]Gano, S., Perez, V., and Renaud, J., "Development and verification of a MATLAB driver for the SNOPT optimization software," Vol. 5, Seattle, WA, United states, 2001, pp. 3212 – 3220.

Appendix

The aircraft parameters for a sample UAV which is used in numerical simulation are presented in Table 2. Table 3 contains the battery pack parameters and the sensor parameters are given in Table 4 .

Table 2. Sample UAV parameters

η_{sol}	$P_{sd}(\frac{W}{m^2})$	$b(m)$	$S(m^2)$	$m(kg)$	η_e	η_{prop}
0.22	380	0.711	0.1566	4.201	0.992	0.7

Table 3. Battery pack (Lithium-Sulfur) parameters

Q	V_{OC}	R	m_{Batt}	$P_{Batt_0,D/C}$
26.4 Ah	12.6 V	0.0125 Ω	1.280 kg	± 30 $watt$

Table 4. Sensor parameters

θ	h_{max}	h_0
30 deg	500 m	750 m